Plasmonics
DOI 10.1007/s11468-015-0153-6

Plasmon-Induced Transparency in a Surface Plasmon Polariton Waveguide with a Right-Angled Slot and Rectangle Cavity

Da-Ming Yu [1] · Xiang Zhai [1] · Ling-Ling Wang [1] · Qi Lin [1] · Hong-Ju Li [1] · Sheng-Xuan Xia [1] · Xiong-Jun Shang [1]

Received: 25 September 2015 / Accepted: 11 December 2015

Abstract The phenomenon of plasmon-induced transparency (PIT) is realized a in surface plasmon polariton waveguide at near-infrared frequencies. The right-angled slot and rectangle cavity placed inside one of the metallic claddings are respectively utilized to obtain bright and dark modes in a typical bright-dark mode waveguide. A PIT transmission spectrum of the waveguide is generated due to the destructive interference between the bright and dark modes, and the induced transparency peak can be manipulated by adjusting the size of the bright and dark resonators and the coupling distance between them. Subsequently, spectral splitting based on the PIT structure is studied numerically and analytically. Simulation results indicate that double electromagnetically induced transparency (EIT)-like peaks emerge in the broadband transmission spectrum by adding another rectangle cavity, and the corresponding physical mechanism is presented. Our novel plasmonic structure and the findings pave the way for new design and engineering of highly integrated optical circuit such as nanoscale optical switching, nanosensor, and wavelength-selecting nanostructure.

Keywords Surface plasmons · Plasmon-induced transparency · Integrated optics devices

✉ Xiang Zhai
kele1110@hnu.edu.cn

[1] Key Laboratory for Micro-Nano Optoelectronic Devices of Ministry of Education, School of Physics and Electronics, Hunan University, Changsha 410082, China

Introduction

EIT is a special and counterintuitive quantum interference effect that happens in a laser-driven atomic system resulting in an extraordinary narrowband transparency window over a wide absorption spectrum of an otherwise opaque medium [1–3]. Because the sharp resonance and steep dispersion could realize in EIT, these systems manifest remarkable potential for slow light and optical data storage [4]. Whereas, applications based on quantum EIT are highly limited by the demanding conditions required to maintain electronic coherence. Therefore, mimicking EIT in classical configurations has attracted tremendous attention, and various schemes have been proposed and demonstrated to display the EIT-like spectral responses [5], e.g. PIT [6, 7], coupled-resonator-induced transparency [8], and metamaterial-induced transparency [9–12]. Nowadays, the use of new techniques to fabricate microstructures to manipulate light has been exciting developments in optical physics [13]. Electromagnetic waves trapped on mental-dielectric interfaces and coupled to propagating free electron oscillations in metals, known as surface plasmon polaritons (SPP), are treated as the most promising method for realization of highly integrated optical circuits by reason of significant overcoming of classical diffraction and controlling of light in a nanoscale domain [14–16]. As a significant plasmonic device, SPP waveguides draw more and more attention due to the better restriction of light with an acceptable propagation length for SPP [17]. SPP waveguides are treated as one of the most promising candidates for the nanoscale manipulation and transmission of light [18]. SPP waveguide-resonator systems provide a pathway for the realization of photonic functionality in metallic nanostructures.

Motivated by the above fundamental studies, in this paper, we would like to realize a PIT phenomenon inside a SPP waveguide configuration with a right-angled slot and rectangle cavity

Published online: 23 December 2015

at mid-infrared frequencies. Our results show that the PIT phenomenon in our designed waveguide system can be acquired based on the dark-bright coupling mechanisms, and the transparency peak can be tuned by adjusting the geometry size of the bright and dark resonators and the coupling distance between them. Besides, to emphasize on the capabilities and better functionality of the introduced PIT structure, compared with the conventional one, a double EIT-like splitter is designed and investigated. Here, we refer to the design based on the above PIT structure as hybrid design.

Model

The considered plasmonic waveguide structure is schematically exhibited in Fig. 1a, which consists of a metal-insulator-metal (MIM) structure with a right-angled slot resonator and a rectangle cavity resonator. This structure is a two-dimensional model, and the materials in the white and blue areas are chosen to be air ($\varepsilon_d = 1.0$) and silver (ε_m), respectively. The dielectric function of silver is characterized by the Johnson and Christy model [19]. The width for the MIM waveguide, right-angled, slot and rectangle cavity is w, and c denotes the coupling distance between the right-angled slot and rectangle cavity resonators. The transverse and longitudinal lengths of the right-angled slot are respectively b, g, and the length of the rectangle cavity is s. If we hope to obtain PIT effect, we need to construct bright and dark state structure in our SPP waveguide system based on the theory in Ref. [20]. In our research, the right-angled slot and rectangle cavity are treated as PIT elements and placed inside one of the metallic claddings (see Fig. 1a). The width of the MIM waveguide w is fixed at 50 nm in the whole paper and much smaller than the incident wavelength; therefore, only the fundamental transverse-magnetic (TM) mode can be supported. SPP waves can be stimulated at the mental-insulator interfaces and restricted in the insulator layer when a TM-polarized plane wave is coupled into the bus waveguide from the left side. The transmission characteristics and field distributions of this plasmonic device are simulated by using finite-difference time-domain (FDTD) method which allows us to straightway take advantage of experimental data for the frequency-dependent dielectric constant of metal such as silver with no approximation. Perfectly matched layer (PML) absorbing boundary conditions are utilized at all boundaries of the simulation domain. The right-angled slot ($g = 250$ nm, $b = 445$ nm) which is filled with air is connected to the air core at one end (see Fig. 1a). As a branch of the core, the right-angled slot can be treated as the bright resonator because it can be excited straightway by the input wave. Rectangle cavity which is also filled by air with $s = 380$ nm length is seen as a dark resonator since it cannot be excited directly by the bus waveguide, namely, it is excited by the bright resonator in fact. Coupling distance c between the right-angled slot and rectangle cavity is 5 nm in our structure.

Simulation Results and Discussion

The above arrangement of geometric parameter is for the flowing three reasons. First, When $c = 5$ nm, the bright and dark resonators are close to each other, near-field coupling between them will occur. Second, such arrangement is chosen to ensure that the resonance wavelength of dark resonance is consistent with that of the bright resonance. Third, the bright resonator displays broad-band resonance excitation and the dark resonator exhibits narrow-band resonance excitation, as shown in Fig. 1b, which is because the coupling coefficient is much larger for the right-angled slot directly connected to the input MIM waveguide, and the rectangle cavity resonator is evanescent coupled to the input MIM waveguide with 5 nm gap.

Therefore, the stop bands of the right-angled slot resonator and the rectangle cavity resonator are overlapped and when the two plasmonic resonators are evanescent coupled with a gap $c = 5$ nm as shown in Fig. 1a, a PIT peak can be formed in the relative broad stop band of the right-angled slot resonator (see Fig. 2a). In other words, the broad resonant mode of the right-angled slot is splitted into two resonant modes, one of them is blue shifted relative to the individual resonator while the other is red shifted (see Figs. 1b and 2a). This phenomenon is analogous to the mode splitting on the basis of the plasmon

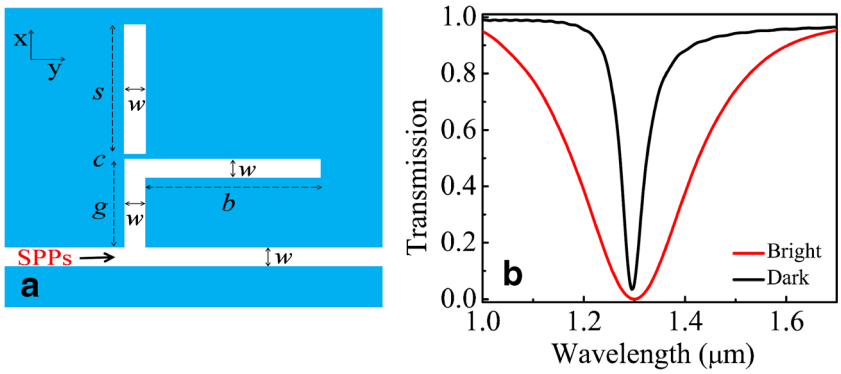

Fig. 1 **a** Schematic diagram and geometric parameters of the nanoscale plasmonic resonator system. **b** The transmission spectrum of bright and dark state, respectively

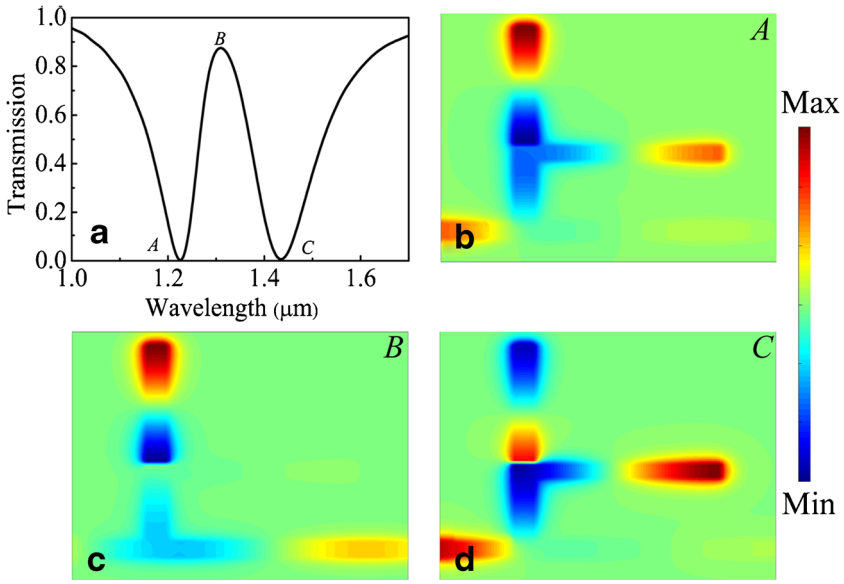

Fig. 2 **a** PIT transmission spectrum of the nanoscale plasmonic resonator system. The H_z field distributions plotted in **b**–**d** corresponding to the characteristic wavelength values denoted by A, B, and C in Fig. 2a, respectively

hybridization theory, which is used in the coupled metal nanoparticle systems [21]. Figure 2b–d shows the H_z amplitude distributions corresponding to the three characteristic wavelengths respectively represented by *A*, *B*, and *C* in Fig. 2a. At the wavelengths λ_A and λ_C, the bright resonator is effectively excited, in the circumstances, most of incident electromagnetic wave energy is strongly reflected by the bright resonator and is leaked into the outer space. Thus, the transmission of the waveguide at wavelengths λ_A and λ_C approaches zero, as demonstrated in Fig. 2a. From the H_z field distributions of the two split resonances, which are shown in Fig. 2a, d, it should be noted that for the split high energy mode, the H_z fields in the coupled cavities are inphase while the H_z fields are antiphase for the low energy mode. Besides, H_z fields are well coupled into the right-angled slot resonator and antiphase with respect to the H_z fields in input MIM waveguides, which induce the destructive interference and transmission suppression. While for the PIT peak or wavelength λ_B, the coupling effect between the bright and dark resonators will result in strong resonance of the dark resonator, and the strong excitation of the dark resonator suppresses the oscillation of the bright resonator in a destructive way. This means that the interaction between bright and dark resonator leads to a weak excitation of bright resonator and a strong excitation of dark resonator, as shown in Fig. 2c. The H_z field distributions in Fig. 2c indicate that the right-angled slot resonator is poorly

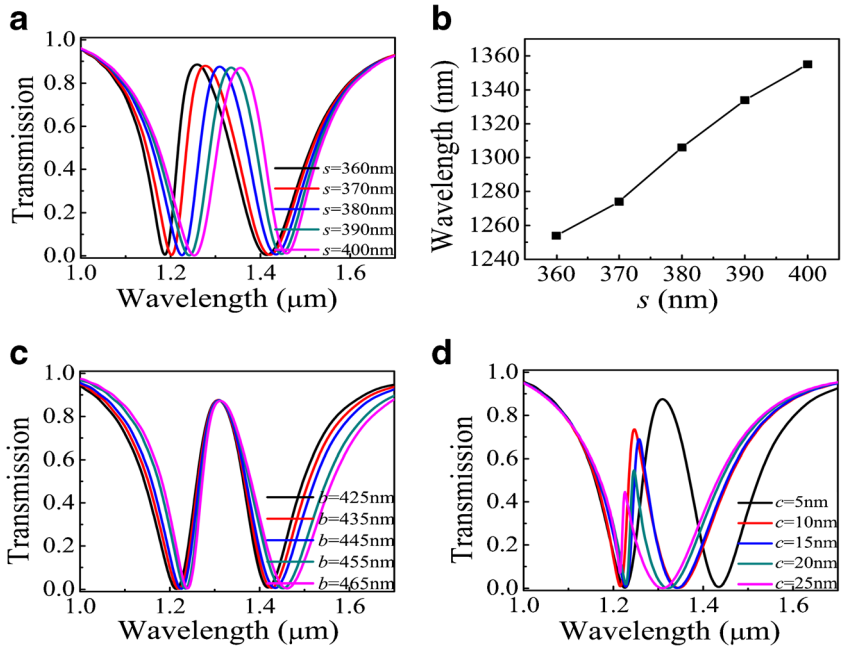

Fig. 3 **a** Transmission spectra for different lengths of the rectangle cavity resonator s ($b = 445$ nm, $g = 250$ nm, $c = 5$ nm). **b** Resonance peak wavelength of the structure versus the length of the rectangle cavity resonator s. **c** Transmission spectra for different length of the right-angled slot b ($g = 250$ nm, $c = 5$ nm, $s = 380$ nm). **d** The transmission spectra for the coupled PIT system with different coupling gap size *c* ($b = 445$ nm, $g = 250$ nm, $s = 380$ nm)

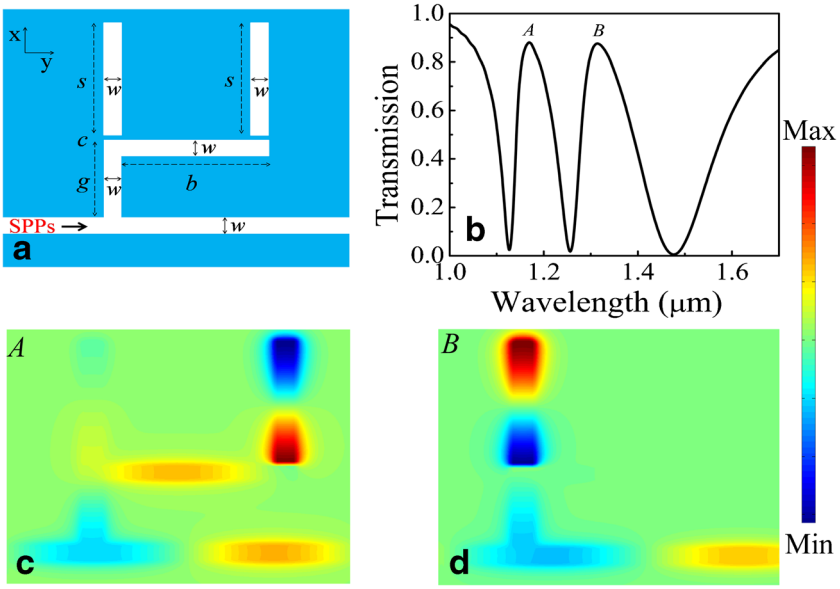

Fig. 4 **a** Schematic diagram and geometric parameters of the two rectangle cavities and a right-angled slot. **b** Transmission spectrum of the two rectangle cavities and a right-angled slot system. The H_z field distributions plotted in **c**–**d** corresponding to the characteristic wavelength values denoted by A and B in Fig. 2b, respectively

coupled and oscillates inphase with the input MIM waveguide, which induces the PIT phenomenon. Therefore, a transmission peak emerges at the wavelength λ_B (see Fig. 2a). We can obviously know that the peak value of transmission spectrum in Fig. 2a is higher than that in Ref. [22], and two dip values are lower than that in Ref. [22].

It is well known that the transmission characteristics of the coupled PIT system can be influenced by the structure parameters. First, we calculated the transmission spectra for different lengths of the rectangle cavity resonator *s* and as shown in Fig. 3a. It is clear that the resonance peak wavelength has a red shift with the increasing length *s*. Fig. 3b displays the relationship between the resonance peak wavelength and the length *s*; it is found that the resonance peak wavelength has an approximate linear relationship with the length *s*. Successively, we research the effect of the length of the right-angled slot resonator *b* on the resonance wavelength and as shown in Fig. 3c. It is obvious that the resonance wavelength almost unchanged with *b* increasing. Furthermore, the effects of the coupling gap size *c* on the PIT spectra are studied and are shown in Fig. 3d. It is evident that the energy gap between two split resonant modes gets smaller when the coupling gap size *c* between the right-angled slot resonator and the rectangle cavity resonator increases. This can be explained by the plasmon hybridization theory that the interactions between the right-angled slot and rectangle cavity resonators get weaker with increasing coupling gap size. Furthermore, when coupling gap size increases, the bandwidth of the PIT decreases because of the decreased energy gap between the two split resonant modes. Therefore, according to the results and analysis, one can easily manipulate the resonance wavelength by changing the length of the rectangle cavity resonator *s* or modifying the coupling gap size *c* between the right-angled slot and rectangle cavity resonators.

The proposed PIT structure in Fig. 1a is very flexible and can be conveniently extended to a double EIT-like system by adding another rectangle cavity, as shown in Fig. 4a. The new rectangle cavity being same with left one in geometric dimensioning is putted on the other end of the right-angled slot, and distance between the right-angled slot and this rectangle cavity is also 5 nm. Such arrangement of parameters of the structure can lead to two transmission peaks, showing two EIT-like optical responses, as shown in Fig. 4b. Afterwards, the corresponding field distributions of H_z at these two transmission peaks are displayed in Fig. 4c, d for the sake of uncovering the reasons of these two peaks. It is simple to understand that Figs. 4d and 2c have the same field distribution at $\lambda = 1312$ nm, hence, propagation

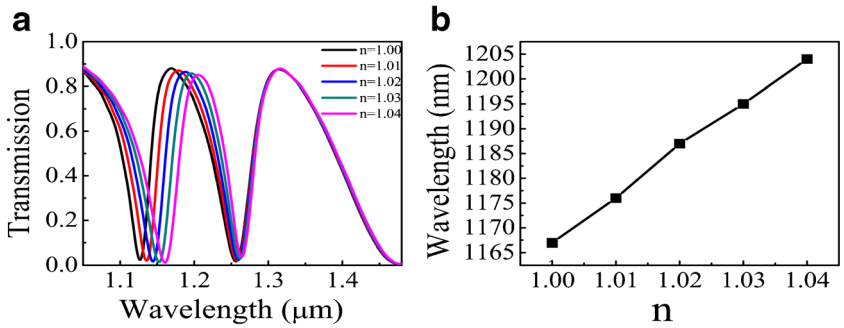

Fig. 5 **a** Transmission spectra for different refractive indexes in the right rectangle cavity in Fig. 4a. **b** Resonance peak wavelength of the structure versus the refractive index in the right rectangle cavity resonator

behavior of SPP for this peak is similar to that of the above PIT structure, and the previous analysis can account for this peak. As to the other peak $\lambda = 1169$ nm, the formation of the peak is due to the near-field coupling effect between the right-angled slot resonator and the right rectangle cavity resonator. The structure in Fig. 4a is a feasible structure which is playing a key role in realization of different integrated optical devices, for example, filters and optical switches.

In addition, we research the impact of the material embedded in the right rectangle cavity in Fig. 4a on the double EIT-like transmission spectrum. It is found that the left center wavelength shows a red shift by altering the refractive index as exhibited in Fig. 5a. The above result can be illustrated by the standing wave theory in Ref. [23]. Even if the model considered here is other than that in Ref. [23], both models have parallel physical mechanism. Figure 5b shows the relationship between the resonance peak wavelength and the refractive index in the right rectangle cavity resonator, it is found that the resonance peak wavelength has an approximate linear relationship with the refractive index. Hence, on the basis of the results and analysis, one can easily control the resonance wavelength by fitting the material with suitable refractive index in the rectangle cavity. Moreover, the suggested model can realize a middling sensitivity nanosensor with the sensitivity of 870 nm/RIU (per unit variations of the refractive index) [24].

Conclusions

In conclusion, the PIT phenomenon has been researched numerically and theoretically in the nanoscale plasmonic waveguide system which consists of a MIM structure with a right-angled slot resonator and a rectangle cavity resonator. The transmission window seems to be nice with a high peak value and two low dip values; meanwhile, the transmission window can be tuned by adjusting the geometry size of the bright and dark resonators and the coupling distance between them. Spectral splitting based on the PIT structure and the influence of the material embedded in the rectangle cavity on the double EIT-like phenomenon have also been researched. The present design thought could find its application in nanoscale optical switching, nanosensor, and nanolaser in highly integrated optical circuits.

Acknowledgments This work was supported by the National Natural Science Foundation of China (Grant Nos. 61505052, 11074069, 61176116).

References

1. Fleischhauer M, Imamoglu A, Marangos JP (2005) Electromagnetically induced transparency: optics in coherent media. Rev Mod Phys 77(2):633
2. Harris SE (2008) Electromagnetically induced transparency. Phys Today 50(7):36–42
3. Boller KJ, Imamoğlu A, Harris SE (1991) Observation of electromagnetically induced transparency. Phys Rev Lett 66(20):2593
4. Phillips DF, Fleischhauer A, Mair A, Walsworth RL, Lukin MD (2001) Storage of light in atomic vapor. Phys Rev Lett 86(5):783
5. Papasimakis N, Fedotov VA, Zheludev NI, Prosvirnin SL (2008) Metamaterial analog of electromagnetically induced transparency. Phys Rev Lett 101(25):253903
6. Kekatpure RD, Barnard ES, Cai W, Brongersma ML (2010) Phase-coupled plasmon-induced transparency. Phys Rev Lett 104(24): 243902
7. Han Z, Bozhevolnyi SI (2011) Plasmon-induced transparency with detuned ultracompact Fabry-Perot resonators in integrated plasmonic devices. Opt Express 19(4):3251–3257
8. Totsuka K, Kobayashi N, Tomita M (2007) Slow light in coupled-resonator-induced transparency. Phys Rev Lett 98(21):213904
9. Zhang J, Xiao S, Jeppesen C, Kristensen A, Mortensen NA (2010) Electromagnetically induced transparency in metamaterials at near-infrared frequency. Opt Express 18(16):17187–17192
10. Tassin P, Zhang L, Koschny T, Economou EN, Soukoulis CM (2009) Low-loss metamaterials based on classical electromagnetically induced transparency. Phys Rev Lett 102(5):053901
11. Liu N, Weiss T, Mesch M, Langguth L, Eigenthaler U, Hirscher M, Giessen H (2009) Planar metamaterial analogue of electromagnetically induced transparency for plasmonic sensing. Nano Lett 10(4): 1103–1107
12. Liu N, Langguth L, Weiss T, Kästel J, Fleischhauer M, Pfau T, Giessen H (2009) Plasmonic analogue of electromagnetically induced transparency at the Drude damping limit. Nat Mater 8(9): 758–762
13. Boyd RW, Gauthier DJ (2006) Photonics: transparency on an optical chip. Nature 441(7094):701–702
14. Zia R, Schuller JA, Chandran A, Brongersma ML (2006) Plasmonics—the wave of chip-scale device technologies. Mater Today 9:20–27
15. Bozhevolnyi SI, Volkov VS, Devaux E, Laluet JY, Ebbesen TW (2006) Channel plasmon subwavelength waveguide components including interferometers and ring resonators. Nature 440(7083): 508–511
16. Barnes WL, Dereux A, Ebbesen TW (2003) Surface plasmon subwavelength optics. Nature 424(6950):824–830
17. Zentgraf T, Zhang S, Oulton RF, Zhang X (2009) Ultranarrow coupling-induced transparency bands in hybrid plasmonic systems. Phys Rev B 80(19):195415
18. Neutens P, Van Dorpe P, De Vlaminck I, Lagae L, Borghs G (2009) Electrical detection of confined gap plasmons in metal–insulator–metal waveguides. Nat Photonics 3(5):283–286
19. Johnson PB, Christy RW (1972) Optical constants of the noble metals. Phys Rev B 6(12):4370
20. Zhang S, Genov DA, Wang Y, Liu M, Zhang X (2008) Plasmon-induced transparency in metamaterials. Phys Rev Lett 101(4): 047401
21. Nordlander P, Oubre C, Prodan E, Li K, Stockman MI (2004) Plasmon hybridization in nanoparticle dimers. Nano Lett 4(5): 899–903
22. Zhang Z, Zhang L, Li H, Chen H (2014) Plasmon induced transparency in a surface plasmon polariton waveguide with a comb line slot and rectangle cavity. Appl Phys Lett 104(23):231114
23. Hu F, Yi H, Zhou Z (2011) Wavelength demultiplexing structure based on arrayed plasmonic slot cavities. Opt Lett 36(8):1500–1502
24. Chen J, Li Z, Yue S, Xiao J, Gong Q (2012) Plasmon-induced transparency in asymmetric T-shape single slit. Nano Lett 12(5): 2494–2498